Bitlis Eren Üniversitesi Fen Bilimleri Dergisi

Numerical Investigation of Mold Heating Power and Time in Metal Layered Composite Production

Muhammed Safa KAMER[1], Arif ÇUTAY[1*], Şemsettin TEMİZ[2], Ahmet KAYA[1]

[1]Kahramanmaraş Sutcu Imam University, Faculty of Engineering and Architecture, Mechanical Engineering Department, Kahramanmaraş, Turkey
[2]Inonu University, Faculty of Engineering, Mechanical Engineering Department, Malatya, Turkey
(ORCID: 0000-0003-3852-1031) (ORCID: 0000-0002-0057-9417) (ORCID: 0000-0002-6737-3720)
(ORCID: 0000-0001-9197-3542)

Abstract

The curing time of epoxy resin is an important phenomenon in the production of metal-layered composites. In this study, the heating time of the mold and epoxy resin was investigated by performing numerical analysis based on time to reduce the curing time. The most consistent mesh structure was chosen among five different mesh numbers in terms of the difference between temperature results. 10 different cases were created to examine different heater powers and different operating patterns. The results were examined by creating a temperature-time graph and contours showing the temperature distribution. As the number of cartridges and heater power increase, higher temperatures are reached in a shorter time. Even with the same heater power, different operating patterns can lead to differences in results in terms of temperature. The different operating pattern was seen as an independent parameter in heater power for obtaining a homogeneous temperature distribution.

1. Introduction

Composite materials have been used in many fields from the past to the present, and they are one of the most important alternatives that can replace traditional materials in terms of lightness and strength [1]-[4]. Composite materials have many advantages over traditional materials as well as disadvantages. The main disadvantages of the use of composite materials can be listed as molding, production time, and production costs. The most important factors affecting production costs are the cost of composite material components and molding costs. The most important factor affecting the production time is the resin curing time. Many experimental and numerical studies have been carried out in the literature to reduce the resin curing time, some of which are given below.

Liu et al. [5] simulated resin transfer molding to observe gate control, venting, and dry spot prediction process. The liquid Injection Molding Simulation program which is based on the finite element technique was used to solve the governing equation of the problem. As a result of simulation, they proved the benefit of numerical simulation in molding processes to make cost-effective manufacturing. Saouab et al. [6] investigated injection simulations of thick composite parts manufactured by the RTM process. Palardy et al. [7] simulated class A surface finish in the resin transfer molding process. Walczyk and Kuppers [8] studied the thermal distribution of composite laminar parts by utilizing COSMOS (Finite Element Analysis (FEA)) in thermal press curing. Pressure uniformity tests were done to validate the results of the FEA study. 12 discrete points of mold were selected to analyze pressure distribution. 32,000 tetragonal elements were created on the curing mold geometry tool surface. Laurenzi et al. [9] simulated a large composite aeronautic beam by resin transfer

---

modeling. The numerical analysis process was carried out with the help of a commercial Mold Flow program. The simulation aims to investigate the resin flow process during impregnation. Finite element-modified control volume analysis was utilized to solve governing equations. Triangular elements were chosen to mesh the discretization process. Mesh analysis was performed to make mesh independency. As a result of the simulation, it is concluded that numerical modeling of the resin transfer process was useful while experimental trial and error should be minimized. Rahman et al.[10] made an optimization study of an inorganic matrix material for high-temperature reinforced composites. They divided the resin into three different stages. As a result of this, it is stated that controlling the duration and humidity was facilitated. Also, improved thermos-dynamic stability was achieved at high temperatures. Keller et al. [11] studied the compression resin transfer molding process in terms of flow and heat transfer. The numerical processes were simulated in COMSOL Multiphysics 5.0 program. A triangular 0.68 mm mesh was utilized in this simulation. Maximum resin temperature was observed at different time intervals while using variable injection pressures. They concluded that the high exothermic reaction of epoxy can be controlled with the utilization of correct manufacturing and processing conditions. Liu et al. [12] studied ohmic heating curing of fiber/carbon nanofiber in an ultralow environment. They conclude that ohmic heating can give comparable results in terms of power and time requirement as compared to other heating methods. Chen et al. [13] monitored the temperature in laminated composite plates by utilizing FBG sensors. The time range required to reach maximum temperature (Nearly 180ºC) was between 255 and 266 min in their experimental study. Li et al. [14] investigated cure-induced temperature gradients in laminated composites in numerical and experimental ways. In this study, they concluded that mold thickness is a significant factor in heating time in laminated composite curing. Maximum temperature was achieved after 140 minutes for laminated composites in this study. Also, 180oC was the maximum temperature at the most heated point in their experimental results. Wu et al. [15] investigated experimentally high-quality plate-shaped A356 alloy casting by a combined ablation cooling and mold heating method. They concluded that the risk of shrinkage porosity can be reduced when the mold temperature is higher than 200 oC. Rosa et al. [16] conducted a CFD study of cyclic transient heating of a blank mold with a conformal channel for manufacturing glass containers. They produced novel blank molds for the glass industry to reduce the operating temperature. 100 C temperature decrease was achieved by a novel blank mold called as ShellMould.

In this study, heater cartridges were added to the pressing mold system used in the production of laminated composites to reduce the curing time of epoxy resin in metal-layered composite production. Thus, the mold and epoxy resin will be heated during the pressing stage in the production of layered composites, and the curing time of the epoxy resin will be reduced. For this purpose, time-dependent numerical analyses were carried out using different heater powers and operating schemes. Thus, the necessary parameters were investigated for the metal-layered composite materials placed between the molds to reach the desired temperature in the shortest time in a homogeneous manner. It has been revealed that some of the parameters determined to be investigated in this and similar studies can also be examined with numerical analysis programs without the need for experimentation. In this way, it is aimed to save time and cost.

2. Material and Method

Reducing the resin curing time in composite material production is important in terms of accelerating composite material production. For this reason, composite materials are first pressed under certain pressures during the production phase, and then the curing of the resin is accelerated by firing. In this study, pressing and heating of the resin were tried to be performed at the same time, thus minimizing the production time of metal-layered composite material was aimed. For this purpose, a mold, press, and external environment used in the production of laminated composite materials were designed in SolidWorks 2018 solid modeling program (Figure 1), and numerical analyzes were carried out in the Fluent module of the Ansys 18.1 program. Ansys Fluent is a proven computational fluid dynamics program that is utilized in the numerical analysis of heat and flow problems [17]-[20].
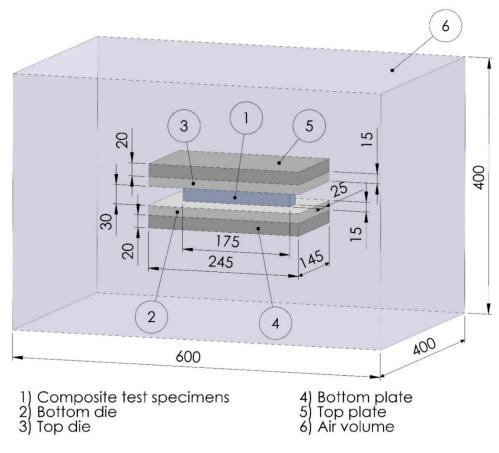
Figure 1. The design used in numerical analysis.

1) Composite test specimens
2) Bottom die
3) Top die
4) Bottom plate
5) Top plate
6) Air volume

To heat the mold and resin during pressing in the production of composite materials, 6mm diameter, 17mm high, cylindrical heater cartridges with cylindrical geometry are placed on the lower plate and upper parts of the press. A total of 120 heater cartridges were utilized, 60 for the lower plate and 60 for the upper press. The layout of the heater cartridges is shown in Figure 2. Heater cartridges are defined to the Ansys-Fluent program in groups of twenty as separate for bottom plate and top press (bottom-inner, bottom-middle, bottom-outer, top-inner, top-middle, top-outer). Thus, in numerical analysis, different heater groups were operated together, and the effect of different heater operating patterns was examined.
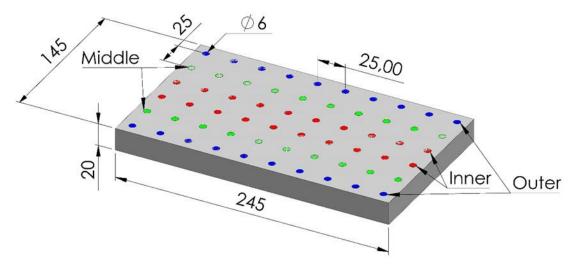

Figure 2. Heater cartridge layout.

Different heater powers and different heater operation patterns used in numerical analyzes are given in Table 1. Numerical analyzes were performed for 9 different cases using different powers and different operating schemes.

Table 1. Heater powers and operating arrangements used in numerical analysis

Numerical analysis ID	Heater cartridge usage status						Heater power (W)	Number of active heaters	Total heater power (W)	Heat flux (W/m^2)
	Bottom plate			Top plate						
	Inner	Middle	Outer	Inner	Middle	Outer				
Case-1	On	On	On	On	On	On	10	120	1200	31206.82
Case-2	On	On	On	On	On	On	20	120	2400	62413.72
Case-3	On	On	On	On	On	On	30	120	3600	93620.55
Case-4	On	On	On	On	On	On	40	120	4800	124827.4
Case-5	On	On	On	On	On	On	50	120	6000	156034.3
Case-6	On	On	On	Off	Off	Off	50	60	3000	156034.3
Case-7	Off	Off	Off	On	On	On	50	60	3000	156034.3
Case-8	On	Off	Off	On	Off	Off	50	40	2000	156034.3
Case-9	Off	On	Off	Off	On	Off	50	40	2000	156034.3
Case-10	On	On	Off	On	On	Off	50	80	4000	156034.3

As a result of numerical analysis, temperature values were taken from 5 different points (Figure 3) on the composite test sample placed between the molds, and the analysis results were compared. At these points, Y=0 and Z=0, and results were obtained such that only the positions of the points on the X-axis changed. In addition, as a result of the analysis, the temperature distribution contours on the composite test sample were also examined.
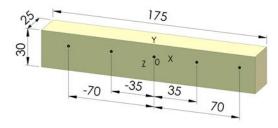

Figure 3. Composite test specimen temperature distribution measurement points.

In analyses using computational fluid dynamics, the correct determination of the solution mesh is of high importance in terms of the accuracy of the result. For this reason, using different variations, 5 different numbers of mesh structures were used to divide the flow volume into elements, and the mesh calculation time, which minimized the difference between the temperature results, was chosen considering the calculation time. Different element sizes and growth rates were given different values in the flow volume and mold, and solution mesh numbers from approximately 5 million to 13 million were created. Mass element dimensions were defined separately for all the masses in the design, and a separate element size definition was made for the part of the air volume between the upper and lower molds. The parameters used in the mesh independence studies are given in Table 2. In these analyses, 0.1s Times step size was used, and 3000 steps were solved. As a result, 300s solutions were obtained as a result of the analysis. Analyzes were performed while the heater cartridges were in the Case-4 state indicated in Table 1.

Table 2. Parameters used in mesh independence studies

Numerical analysis ID	Body element size (mm)					Grow rate	Number of mesh element	Max. Skewness	Min. Orthogonal quality
	Composite test specimens	Top and Bottom dies	Top and Bottom plates	Air volume	Air volume between dies				
Mesh-1	5	5	5	10	10	1.1	4,996,595	0.799	0.2
Mesh-2	2	5	5	10	2	1.1	6,542,234	0.799	0.2
Mesh-3	**2**	**2**	**2**	**10**	**10**	**1.2**	**7,622,720**	**0.83888**	**0.16112**
Mesh-4	2	2	2	5	5	1.2	11,519,731	0.82295	0.17705
Mesh-5	2	2	2	5	5	1.1	12,910,476	0.8225	0.17744

The results obtained from the mesh independence studies are given in Table 3. For each analysis, temperature values were taken from the points indicated in Figure 3 and the average of these temperature values was calculated and a table was created. When Table 3 is examined, it is seen that the results obtained from the mesh independence studies are very close to each other. For this reason, it was decided to use the solution mesh with the number of 7.6 million elements in the calculations with the most accurate result without increasing the calculation time and load too much (Mesh-3). In addition, numerical analyses were carried out at different time step size times (0.01s; 0.05s; 0.1s) using the selected mesh structure, and 300s solutions were obtained as a result

of these analyses. The results obtained from the analysis are also given in Table 3. It is seen that the results obtained from time step size independence studies are also very close to each other, and in the following analyses (other cases specified in Table 1), Mesh-3 mesh structure, 0.1s time step size, and 3000-time step were used. The Mesh-3 mesh used in the numerical calculation is shown in Figure 4.

In the numerical calculation, in the nozzle design provided by the die heating, the inlet boundary condition was created by giving the heat flux to the wall boundary condition, and the pressure boundary condition was chosen as the atmospheric boundary condition at the outlet. The type of flow was chosen as laminar due to the nature of the problem.

Table 3. Results obtained from the studies of independence from mesh and time step

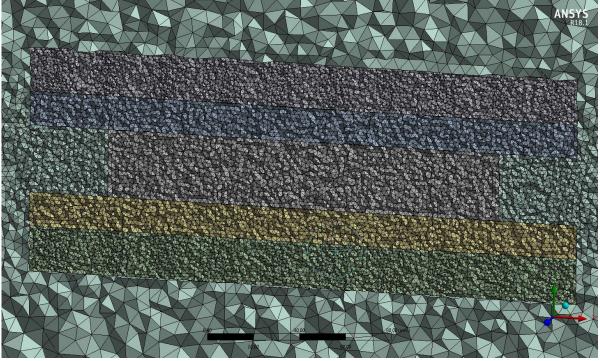| Numerical analysis ID	Temperature (K)									
	30s	60s	90s	120s	150s	180s	210s	240s	270s	300s
Mesh-1	310.21	326.01	342.78	359.82	376.94	394.08	411.32	428.41	445.40	462.74
Mesh-2	310.20	326.01	342.78	359.88	376.94	394.08	411.24	428.41	445.57	462.74
Mesh-3	**310.37**	**326.23**	**343.02**	**360.06**	**377.18**	**394.33**	**411.49**	**428.65**	**445.82**	**462.98**
Mesh-4	310.38	326.25	343.04	359.96	377.20	394.35	411.51	428.67	445.84	463.01
Mesh-5	310.37	326.23	343.02	360.06	377.18	394.33	411.49	428.66	446.02	462.99
Time Step Size 0.01s	310.36	326.23	343.02	360.06	377.18	394.32	411.48	428.65	445.81	462.97
Time Step Size 0.05s	310.37	326.23	343.02	360.06	377.18	394.33	411.33	428.65	445.82	462.98

Figure 4. Mesh structure used in numerical studies.

3. Results and Discussion

In this study, the heating time and the maximum temperature are studied using numerical methods depending on time using different heater powers and nozzle configurations. The results are shown graphically and contoured in the figures below. Graphs showing the change of temperature over time are shown for 5 minutes of simulation for 5 different points (-70, -35, 0, 35, 70 mm) averages. Figure 5 (a) shows the time-dependent variation of the average temperature at the 5 different points with all nozzles open at 5 different heater powers. As expected, the highest heater power reaches the highest temperature value in the specified period in the Kelvin temperature unit. It is seen in the graphs that the effect of increasing heater power on temperatures increases over time. Increasing the heater power from 1200W to 6000W causes a 53.6% increase in the maximum temperature that will occur after 5 minutes. The maximum temperature value reached for 6000W was calculated as 504.583 K as a result of numerical simulations. The rate of increase between maximum and minimum power is calculated as 53.3% at the end of the 5 minutes. When the heater power is increased from 1200W to 2400W, the increase in Kelvin from the temperature value is calculated as 11.9%. The temperature difference between different heater power cases increases with time. The maximum temperature that can be reached for case 1 was calculated as 341 K, while case 5 passed this

temperature in 120 seconds. Each 1200W heater power causes an increase of approximately 40 K maximum temperature, while this value is calculated as 50 K when increased from 4800 W to 6000 W. More heater power enables reaching the desired temperature in a shorter time and rising to higher temperatures as expected in our design.

In Figure 5(b), the time-dependent variation of the average temperature for 5 points is shown for 5 different operating cartridge patterns. In these cases, the heater power is changed while using different operating patterns. Even though similar heater powers were studied, the change in heater cartridge positions caused a significant difference in the average temperature graph. The maximum temperature reached by the lowest heater power, 367 K, reached case 5 in less than 120 seconds. Although the increased heater power is increased by using different heater patterns, it enables it to reach higher temperatures in a shorter time. Increasing the heater power from 2000W to 4000W increases the maximum achievable temperature for these cases by 17.95 %. Switching from the heater power of 4000 W to Case 5 is observed in the graph as an approximately 14.28 % increase in the maximum temperature. Although Case 8 and 9 have the same heating power, Case 8 appears to reach higher temperatures in a shorter time. Because while the middle heater cartridges are open in case 9, case 8 has an arrangement in which the inner heater cartridges are opened.
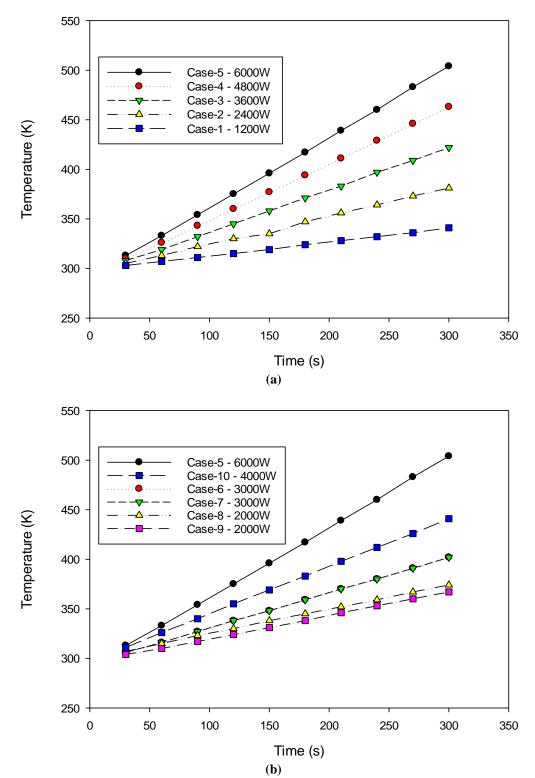
(a)

(b)

Figure 5. Temperature-time graphs created by numerical analysis results using different heater powers (a) and different operating patterns (b).

Figure 6 depicts the temperature contour as user-specified and local cases for different heater power at the end of 300 seconds. The minimum and maximum temperature is specified as 340K and 510 K. In the local case, the temperature is set only for the maximum and minimum values of these cases. For

this reason, there are color differences among contours. The effect of increased heater power on the temperature distribution is clearly shown in the contours created with the user-specified. The local contours depict in terms of color how the open and closed cartridge positions affect the maximum and minimum temperatures that will occur. As the temperature increases at the edge of the mold, a significant decrease towards the middle has occurred as a result of numerical analysis. Figure 7 shows the temperature contour as user-specified and local cases for different heater operating patterns at the end of 300 seconds. The effect of the increased heater power on the temperature is seen in the user-specified contours. The effect of the positions of the opened heater cartridges can be seen in the locally created contours. As expected, as seen in case 6, a temperature increase is observed close to that region when the lower cartridge is open, while a temperature increase is observed in the upper region when the upper cartridge is open. As it can be understood from these contours, besides the heater power, the position of the heater cartridges to be opened is a significant factor in obtaining a homogeneous temperature distribution. Figure 8 shows the temperature distribution of the analysis region from the top view using lower and upper separate operating patterns for XY and YZ planes. As expected, when all heater powers are turned on at the highest level, the amount of red area indicating the height of the temperature covers a lot of space for case 5 compared to the others for both planes. Case 7, where the top heater cartridges are opened, is compared to case 6, where only the bottom cartridges are opened, it seems for this mold design that case 7 affects a larger area in terms of heat increase. In addition, the areas close to the open heater cartridges in the mold show higher values in terms of temperature as expected.
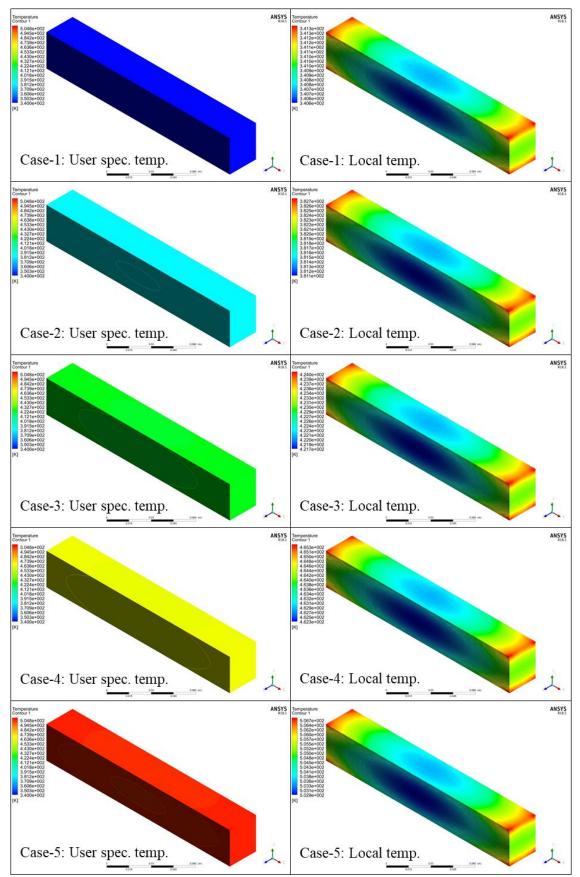
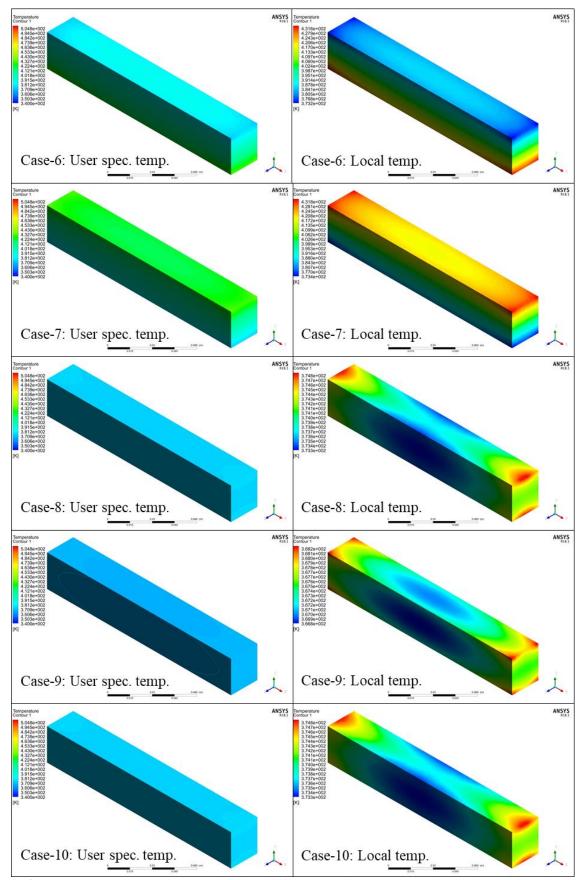**Figure 6.** Temperature contours results using different heater powers and created on test samples.

Figure 7. Temperature contours results using different operating patterns and created on test samples.
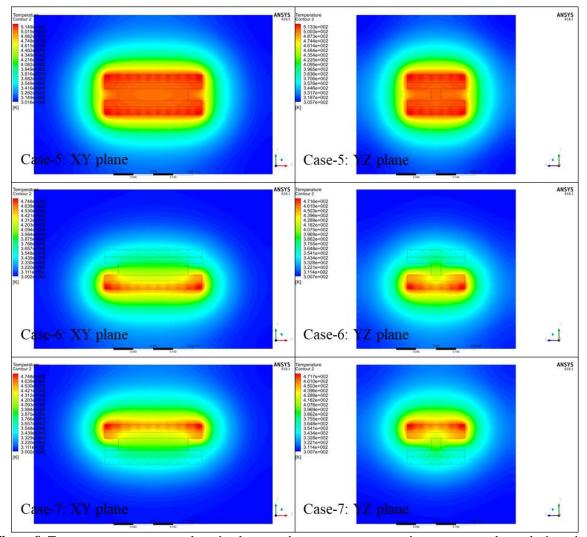
Figure 8. Temperature contours results using lower and upper separate operating patterns on the analysis region.

4. Conclusion

In this study, numerical simulation was performed at laminated composites in order to reduce the curing time of epoxy resin in metal layered composite production for different heater power and different operating patterns. According to different heater power and operating patterns, 10 different situations were created and analyzes were performed. The outputs obtained according to these numerical analyzes are as follows.

- The increased heater power causes higher temperatures to be reached in a shorter time, regardless of the different operating patterns.
- It is seen that choosing the heater cartridges according to the area to be heated provides more effective results.
- For this design, opening the upper heater cartridge provides a temperature increase in a wider area and it is seen to be more efficient.

- Although cases 8 and 9 have the same heater power, case 8 produced higher temperature results. This shows the importance of the heating pattern even though they are of the same power.
- Although case 5 differs from all other cases in terms of reaching higher temperatures in a shorter time, its use according to the desired temperature amount of time may cause unnecessary energy consumption.
- It is important to establish the operating pattern correctly to obtain a homogeneous temperature distribution.

Acknowledgment

Contributions of the authors

All the authors have accepted responsibility for the entire content of this submitted manuscript and approved the submission.

Conflict of Interest Statement

The authors declare no conflicts of interest regarding this article.

Statement of Research and Publication Ethics

The study is complied with research and publication ethics.

References

[1] S. Kaveloğlu and Ş. Temiz, "An experimental and finite element analysis of 3D printed honeycomb structures under axial compression," *Polymers & Polymer Composites*, vol. 30, p. 096739112211223, Jan. 2022.

[2] A. Saylik and Ş. Temiz, "Low-speed impact behavior of fiber-reinforced polymer-based glass, carbon, and glass/carbon hybrid composites," *MP MATERIALPRUEFUNG - MP MATERIALS TESTING*, vol. 64, no. 6, pp. 820–831, Jun. 2022.

[3] S. Kaveloğlu, Ş. Temiz, O. Doğan, and M. S. Kamer, "Investigation of Bending Strength of Honeycomb Sandwich Structures with Different Cell Diameters Produced by 3D Printer," *Çukurova Üniversitesi Mühendislik Fakültesi Dergisi*, vol. 37, no. 2, pp. 459–470, Jun. 2022.

[4] M. Yilmaz, N. F. Yilmaz, and M. F. Kalkan, "Rheology, crystallinity, and mechanical investigation of interlayer adhesion strength by thermal annealing of polyetherimide (PEI/ULTEM 1010) parts produced by 3D printing," *Journal of Materials Engineering and Performance*, vol. 31, no. 12, pp. 9900–9909, Jun. 2022.

[5] B. Liu, S. Bickerton, and S. G. Advani, "Modelling and simulation of Resin Transfer Moulding (RTM)—gate control, venting and dry spot prediction," *Composites Part A: Applied Science and Manufacturing*, vol. 27, no. 2, pp. 135–141, 1996.

[6] A. Saouab, J. Bréard, P. Lory, B. Gardarein, and G. Bouquet, "Injection simulations of thick composite parts manufactured by the RTM Process," *Composites Science and Technology*, vol. 61, no. 3, pp. 445–451, 2001.

[7] G. Palardy, P. Hubert, E. Ruiz, M. Haider, and L. Lessard, "Numerical simulations for class A surface finish in resin transfer molding process," *Composites Part B: Engineering*, vol. 43, no. 2, pp. 819–824, 2012.

[8] D. Walczyk and J. Kuppers, "Thermal press curing of Advanced Thermoset Composite Laminate Parts," *Composites Part A: Applied Science and Manufacturing*, vol. 43, no. 4, pp. 635–646, 2012.

[9] S. Laurenzi, A. Casini, and D. Pocci, "Design and fabrication of a helicopter unitized structure using resin transfer molding," *Composites Part A: Applied Science and Manufacturing*, vol. 67, pp. 221–232, 2014.

[10] A. S. Rahman and D. W. Radford, "Cure cycle optimization of an inorganic polymer matrix material for high-temperature fiber reinforced composites," *Composites Part A: Applied Science and Manufacturing*, vol. 85, pp. 84–93, 2016.

[11] A. Keller, C. Dransfeld, and K. Masania, "Flow and heat transfer during compression resin transfer molding of highly reactive epoxies," *Composites Part B: Engineering*, vol. 153, pp. 167–175, 2018.

[12] Y. Liu, M. Wang, W. Tian, B. Qi, Z. Lei, and W. Wang, "Ohmic heating curing of carbon fiber/carbon nanofiber synergistically strengthening cement-based composites as repair/reinforcement materials used in ultra-low temperature environment," *Composites Part A: Applied Science and Manufacturing*, vol. 125, p. 105570, 2019.

[13] J. Chen, J. Wang, X. Li, L. Sun, S. Li, and A. Ding, "Monitoring of temperature and cure-induced strain gradient in a laminated composite plate with FBG sensors," *Composite Structures*, vol. 242, p. 112168, 2020.

[14] X. Li, J. Wang, S. Li, and A. Ding, "Cure-induced temperature gradient in laminated composite plate: Numerical simulation and experimental measurement," *Composite Structures*, vol. 253, p. 112822, 2020.

[15] J. Wu, D. Sui, and Q. Han, "High quality plate-shaped A356 alloy casting by a combined ablation cooling and mold heating method," *Journal of Materials Processing Technology*, vol. 303, p. 117536, 2022.

[16] N. Rosa, J. Costa, and A. G. Lopes, "CFD study of transient heating and cooling of a blank mold with a conformal cooling channel for manufacturing glass containers," *Results in Engineering*, vol. 17, p. 100932, 2023.

[17] T. Karataş and İ. G. Aksoy, "Heat and Flow Analysis of Different Type Baffle in Shell and Tube Heat Exchanger," *Bitlis Eren Üniversitesi Fen Bilimleri Dergisi*, vol. 10, no. 3, pp. 973–986, 2021. doi:10.17798/bitlisfen.872465

[18] M. Yavuz, C. Yıldız, and G. Çakmak, "Numerical Analysis of Velocity and Temperature Distributions in Winter Air Conditioning of Cabin Type Offices," *Bitlis Eren Üniversitesi Fen Bilimleri Dergisi*, vol. 10, no. 3, pp. 958–972, 2021.

[19] S. Akçay, "Investigation of effects of Baffle Heights on flow and heat transfer in a trapezoidal channel with vertical baffles," *Bitlis Eren Üniversitesi Fen Bilimleri Dergisi*, vol. 11, no. 2, pp. 478–489, 2022. doi:10.17798/bitlisfen.1033852

[20] Y. Sayan, "Investigation of the effect of a different trapezoidal inclination angle in a reverse trapezoidal cross-section flow channel on the performance of the PEM fuel cell with the computational fluid dynamic (CFD) method," *Kahramanmaraş Sütçü İmam Üniversitesi Mühendislik Bilimleri Dergisi*, https://jes.ksu.edu.tr/en/pub/issue/77849/1180483 (accessed Aug. 15, 2023).